INFLUENCE OF FRICTION DEVICES ON THE NONLINEAR SEISMIC RESPONSE OF STEEL STRUCTURES

A. Elenas[1] and D. Tzourmakliotou[2]

[1] *Assoc. Professor, Democritus Univ. of Thrace, Department of Civil Engineering, GR-67100 Xanthi, Greece*
Email: elenas@civil.duth.gr
[2] *Lecturer, Democritus Univ. of Thrace, Department of Civil Engineering, GR-67100 Xanthi, Greece*
Email: dimitratz@gmail.com

ABSTRACT:

This paper investigates the influence of friction devices on the nonlinear seismic response of steel structures. For this purpose a steel frame structure is designed according to the rules of the recent Eurocodes. Four frame types are investigated: type 0 (frame without friction devices), type 1 (friction devices only in the ground level), type 2 (friction devices in all the stories), type 3 (friction devices in all the stories except the ground level). The devices are placed as diagonal trusses in the middle bay of the frame. They are realized as slotted bolt connections. Alternative friction forces are considered. Nonlinear dynamic analyses are carried out for the evaluation of the structural response. The focus is on the maximum inter-story drift ratio (MISDR), which among the several response parameters is chosen as damage index. A set of natural accelerograms is used as seismic excitation for the analysis. Numerical results expose that friction devices reduce the seismic response of steel structures with appropriate number of devices and a sufficient amount of friction forces. Alternative calculations furnish the optimum topology for the devices and the corresponding amounts of friction forces. The mean MISDR is reduced in the optimal case up to 57%, in comparison to the response of the frame without damping devices. Extreme values of the MISDR are also reduced, with a reduction percentage greater than 50%. Thus, friction devices can be used for the preseismic strengthening or postseismic rehabilitation of steel structures.

KEYWORDS: Friction devices, steel structures, energy dissipation

1. INTRODUCTION

In the two latter decades friction devices developed, with increasing importance, to an essential element for the rehabilitation of seismic damaged buildings and for the preventive protection of new building against a seismic impact. The favorable effect of the absorbers is based on the dissipation of a part of the seismic energy that acts on the earthquake-excited construction. The friction absorbers exhibit rectangular loops in the force-deformation diagram during cyclic loads. These are typical for the coulomb friction. A multiplicity of friction absorbers is designed by the industry, which are effectively used in practice. The employment of the energy dissipation elements in a frame structure can be realized alternatively by diagonally or X-shaped trusses [Constantinou et al., 1998], [Hanson et al., 2001], [Li et al., 1995].

For the description of the structural damage status after an earthquake, global damage indicators have been proved satisfactorily. In this paper the maximum inter-story drift ratio is used. By means of numeric simulations the interrelation degree between the dissipation mechanisms and the used global damage indicator is evaluated. This takes place under consideration of the alternative positions and friction forces of the absorbers. The numeric investigation occurs on a ten-story steel frame (with and without absorbers), designed according to the rules of the Eurocodes 3 and 8. The favorable effect of the friction absorbers follows from the comparison of the results with them of the original state (framework without absorbers).

2. FRICTION DEVICES

Friction absorbers are devices, which increase the hysteretic energy dissipation of a building. This additional dissipation is realized due to the friction energy, which is developed in friction surfaces between the constituent elements of the absorbers. Different designs of the friction absorbers were used both to the effective rehabilitation of seismically damaged buildings and for the preventive contribution in new buildings against seismic impact. As examples are here mentioned the systems of Pall, of Sumitomo Metal Ltd. and of Tekton Arizona [Hanson et al., 2001]. Additionally, several materials can be applied for the construction of the friction surfaces (e.g., steel or brass).

In this paper the friction absorbers suggested by Fitzgerald et al. [Fitzgerald et al., 1989] are used, where the energy dissipation mechanism is realized by slotted bolt connections. The dissipation device exhibits rectangular shaped hysteretic loops in the force-deformation diagram during cyclic loads. These loops are typical for the coulomb friction. Their hysteretic behavior is independently from the load frequency and the number of load cycles. Figure 1 shows the construction principle of the used friction devices [Butterworth, 1999]. Figure 2 depicts the hysteretic behavior of friction devices [Li et al., 1995], exposing the influence of different friction surface materials (steel and brass).

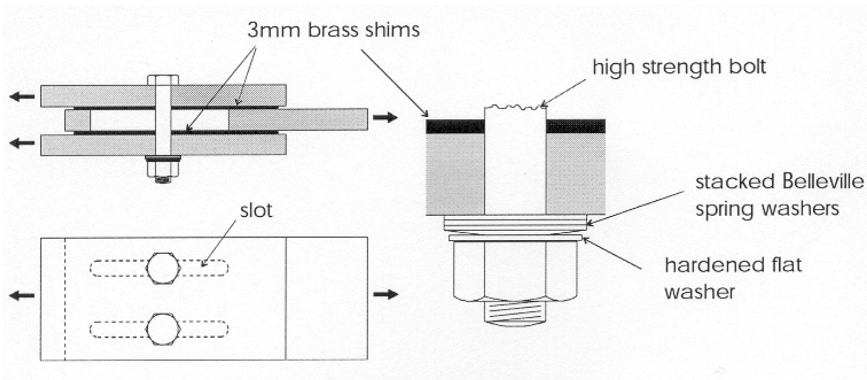

Figure 1. Friction device with slotted bolt connections [Butterworth, 1999]

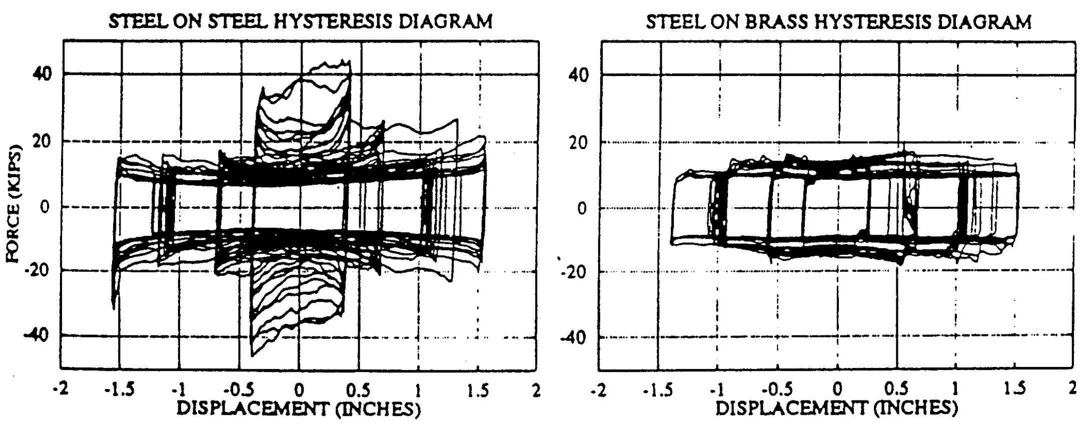

Figure 2. Hysteretic behavior of friction devices [Li et al., 1995]

3. NUMERICAL MODELING

The general differential equation of motion for a multi-degree-of-freedom system under seismic excitation is given by relation (1):

$$\underline{\mathbf{M}}\,\ddot{\underline{\mathbf{u}}} + \underline{\mathbf{C}}\,\dot{\underline{\mathbf{u}}} + \underline{\mathbf{R}}(\underline{\mathbf{u}}) + \underline{\mathbf{F}}_D(\underline{\mathbf{u}}) = -\,\underline{\mathbf{M}}\,\underline{\mathbf{I}}\,\ddot{u}_g + \underline{\mathbf{L}} + \underline{\mathbf{L}}_T \qquad (1)$$

where, $\underline{\mathbf{M}}$ the mass matrix, $\underline{\mathbf{C}}$ the damping matrix, $\underline{\mathbf{R}}$ the nonlinear out-of-balance load vector, $\underline{\mathbf{F}}_D$ the vector of additional damping forces (friction devices), $\underline{\mathbf{u}}$ the displacement vector, $\underline{\mathbf{I}}$ the column vector that contains the displacements of the degrees of freedom due to a unit displacement of the support in the direction of the seismic action, u_g the support displacement due to an earthquake, $\underline{\mathbf{L}}$ the time-independent load vector and $\underline{\mathbf{L}}_T$ the time-dependent load vector.

The additional damping loads from relation (1) are evaluated for friction devices from the following relation:

$$\underline{\mathbf{F}}_D(\underline{\mathbf{u}}) = \underline{\mathbf{D}}\,\underline{\mathbf{F}}_{Di}(\underline{\mathbf{u}}) \qquad (2)$$

where, $\underline{\mathbf{D}}$ the position matrix of the damping devices and $\underline{\mathbf{F}}_{Di}$ the vector with the corresponding damping force of the device (i).

The damping force F_{Di} of the device (i) is defined by the relations (3a) and (3b).

Before sliding begins:

$$F_{Di} = k_{Di} u_i \qquad (3a)$$

when $|F_{Di}| \leq \mu_{Di,HR}\, N_i$.

After sliding begins:

$$F_{Di} = \mu_{Di,GR}\, N_i \qquad (3b)$$

when $\mu_{Di,GR}\, N_i \leq |F_{Di}| < \mu_{Di,HR}\, N_i$,

where: k_{Di} the stiffness, u_i the relative displacement, $\mu_{Di,HR}$ the static coefficient of friction, N_i the force normal to the friction surface, $\mu_{Di,GR}$ the kinematic coefficient of friction, of the respective damper (i).

The nonlinear equation (1) is, under consideration of the relations (2), (3a) and (3b), to be solved. This can be realized with direct time integration methods (e.g. Newmark method) and iteration in each integration step for optimization of the solution (e.g. Newton/Raphson method).

4. DAMAGE INDICATOR

In the present investigation comes to application the maximum inter-story drift ratio (MISDR) as global damage indicator. This index is simple to calculate and characterize both the structural and the architectural (nonstructural) damage satisfactorily. Observations of building damage after strong earthquakes and numerical investigations manifest the effectiveness of this indicator [Elenas and Meskouris, 2001]. Inter-story drift is the relative displacement of one story relative to the other. Here, the inter-story drift is noticed as u. The relationship (1) defines the maximum inter-story drift ratio (MISDR) as the ratio of the maximum absolute inter-story drift $|u|_{max}$ to the inter-story height h:

$$\mathrm{MISDR} = \frac{|u|_{max}}{h} 100\ [\%] \tag{4}$$

5. APPLICATION

The steel frame structure shown in Figure 3 has been detailed according to the rules of Eurocodes 3 (EC3) und 8 (EC8). The slab thickness is chosen equal to 20 cm. The distances between each frame of the structure are equal to 6 m, while the ground floor has a 5 m height and all subsequent floors 4 m. Furthermore, according to Eurocode 8 the subsoil was of type "B" (deep deposits of medium dense sand or over consolidated clay at least 70 m thick), the importance class of the building is "III" and the ductility class is "M". This procedure, apart from the self-weight, has taken into account the snow, the wind and the live loads. The eigenperiod of the frame was 2.68 s.

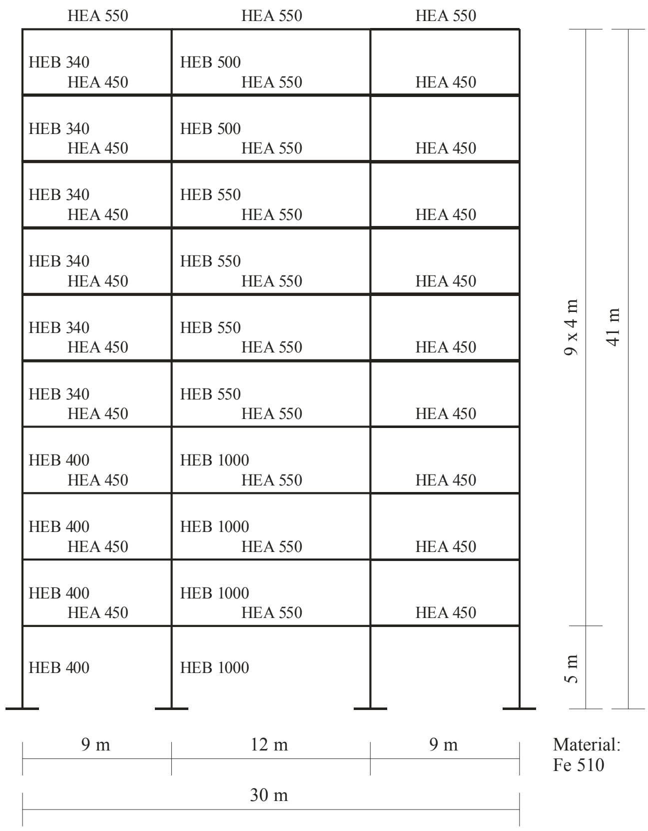

Figure 3. Ten-story steel frame building

After the detailing procedure, follows the realization of a nonlinear dynamic analysis for the evaluation of the seismic response of the structure. For this purpose the program IDARC is applied [Valles et al., 1996]. This solves the equation (1) with the direct time integration procedure after Newmark, combined with the iterative method after Newton/Raphson. A bilinear elasto-plastic model with a hardening of 5% after yielding, models the moment-curvature relationship of the steel cross sections. The yielding curvature corresponds to the condition, where a fiber of the cross section reaches the yield point. The ultimate curvature is defined as the smaller value, either of the curvature that corresponds to the full plastic section condition or the condition where any fiber of the cross section reaches the ultimate strain ($\varepsilon_u = 22\%$).

This investigation uses linked slotted bolts as energy dissipating mechanisms. The prestressed steel screws are in such a manner designed that they develop different friction forces at the contact surfaces: 100 kN, 250 kN, 500 kN, 750 kN and 1000 kN. The force-deformation behavior of the friction absorber is approximated by a bilinear model (Coulomb). Computations have been realized for the optimization of the positioning of the damping devices and their damping forces. The investigation uses four frame types: type 0 (frame without damping devices), type 1 (with damping devices only in the ground floor), type 2 (with damping devices in all stories) and type 3 (with damping devices all stories except in the ground floor). In all cases the friction absorbers are placed as diagonal trusses in the middle bay of the frame. The recorded accelerograms according to Table 1 were used as seismic excitations in the dynamic analyses. Among the several response parameters, the focus is on the MISDR, defined by relation (4), as an overall structural damage indicator (OSDI).

Table 1. Data of the used accelerograms

Nr.	Earthquake	Country	Date	Station	Component	Nr.	Earthquake	Country	Date	Station	Component
1	San Fernando	USA	9/2/1971	No.279	S16E	34	San Salvador	Salvador	10/10/1986	NO.90014	90
2	San Fernando	USA	9/2/1971	No.279	S74W	35	San Salvador	Salvador	10/10/1986	NO.90014	90
3	San Fernando	USA	9/2/1971	No. 279	S74W	36	San Salvador	Salvador	10/10/1986	NO.90016	180
4	Northridge	USA	17/1/1994	Jensen	292	37	San Salvador	Salvador	10/10/1986	NO.90018	0
5	Oroville Aftershock 6	USA	6/8/1975	USGS 0001	N00E	38	Hokkaido	Japan	23/4/1962	SMAC-A	NS
6	Imperial Valley	USA	15/10/1979	USGS 0958	S40E	39	Hokkaido	Japan	23/4/1962	SMAC-A	EW
7	Imperial Valley	USA	15/10/1979	USGS 5054	S40E	40	Hokkaido	Japan	23/4/1962	SMAC-A	UD
8	Central California	USA	4/9/1972	USGS 1211	N29W	41	Hokkaido	Japan	5/4/1966	DC-3C	EW
9	Northridge	USA	17/1/1994	USC# 0055	N90E	42	Hokkaido	Japan	19/11/1967	SMAC-A	NS
10	Imperial Valley	USA	15/10/1979	USGS 5165	N	43	Hokkaido	Japan	19/11/1967	SMAC-A	EW
11	Northridge	USA	17/1/1994	USC# 0003	S00E	44	Hokkaido	Japan	1/4/1968	SMAC-B2	NS
12	Imperial Valley	USA	15/10/1979	USGS 0958	S50W	45	Hokkaido	Japan	1/4/1968	SMAC-B2	EW
13	Northridge	USA	17/1/1994	USC# 0013	N09E	46	Athens	Greece	7/9/1999	NO.081	L
14	Northridge	USA	17/1/1994	USC# 0056	N46E	47	Athens	Greece	7/9/1999	NO.117	T
15	Imperial Valley	USA	18/5/1940	No. 117	S00E	48	Athens	Greece	7/9/1999	NO.140	L
16	Imperial Valley	USA	15/10/1979	USGA 0942	S40E	49	Athens	Greece	7/9/1999	NO.140	T
17	Imperial Valley	USA	15/10/1979	USGA 5028	S40E	50	Kalamata	Greece	13/9/1986	Kalamata O.T.E.	L
18	San Fernanto	USA	9/2/1971	No. 128	N69W	51	Kalamata	Greece	13/9/1986	Kalamata O.T.E.	T
19	Loma Prieta	USA	18/10/1989	Appeel Array	43	52	Kalamata	Greece	15/9/1986	Kalamata O.T.E.	L
20	San Fernando	USA	9/2/1971	No.122	S70E	53	Korinthos	Greece	24/2/1981	Kalamata O.T.E.	L
21	San Fernando	USA	9/2/1971	No.110	N69W	54	Korinthos	Greece	24/2/1981	Korinthos O.T.E.	T
22	Loma Prieta	USA	18/10/1989	Emerville	260	55	Korinthos	Greece	25/2/1981	Korinthos O.T.E.	L
23	Loma Prieta	USA	18/10/1989	Hollister	180	56	Korinthos	Greece	25/2/1981	Korinthos O.T.E.	T
24	Imperial Valley	USA	15/10/1979	USGS 0942	S50W	57	Bucharest	Rumania	4/3/1977	INCERC	N270
25	Kobe	Japan	17/1/1995	Kobe	EW	58	Bucharest	Rumania	4/3/1977	INCERC	N0
26	Kobe	Japan	17/1/1995	Kobe	NS	59	New Mexico	Mexico	8/5/1996	SCT1	S00E
27	Erzincan Met.	Turkey	13/3/1992	Erzincan	EW	60	New Mexico	Mexico	19/9/1985	SCT1	N90W
28	Erzincan Met.	Turkey	13/3/1992	Erzincan	NS	61	Loma Prieta	USA	17/10/1989	NO.57007	90
29	Dursunbey Kandilli	Turkey	18/7/1979	Dursunbey	EW	62	Loma Prieta	USA	17/10/1989	NO.57007	0
30	San Salvador	Salvador	10/10/1986	No. 90005	270	63	Petrolia	USA	25/4/1992	NO.89156	90
31	San Salvador	Salvador	10/10/1986	NO.90006	180	64	Petrolia	USA	25/4/1992	NO.89156	0
32	San Salvador	Salvador	10/10/1986	NO.90013	90	65	Loma Prieta	USA	17/10/1989	No.58135	90
33	San Salvador	Salvador	10/10/1986	NO.90014	90	66	Loma Prieta	USA	17/10/1989	No.58135	0

6. RESULTS

The results of the numerical investigation of the four frame types are presented as bar charts in Figure 4. The abscissa represents the frame type and the friction force of the absorbers. The ordinates give the extreme values and the average values of MISDR for the 66 examined natural accelerograms as provided in Table 1. A condition for the damage-reducing effect is however that a sufficient number of energy dissipating mechanisms are present. Good solutions represent the frame types 2 (friction absorbers in all stories available) and 3 (friction devices available in all stories except in the ground floor), with a friction force for each device of 500 kN, 750 kN and 1000 kN. The mean value of maximum inter-story drift ratios (MISDR) reduces from the value 1.55% for the frame type 0 (frame without friction absorbers) to 0.875% for the frame type 3 and a friction force of 750 kN. Figure 4 shows also that the extreme values of the MISDR, 6.33% and 0.23% (type of framework 0), drop on the values 3.63% (type of framework 2, 500 kN) and 0.12% (framework types 2 and 3, 750 kN and 1000 kN). Finally, Figure 4 exposes that the absorber presence leads not always in a MISDR decrease (mean value of MISDR for frame type 1, 500 kN, 750 kN and 1000 kN).

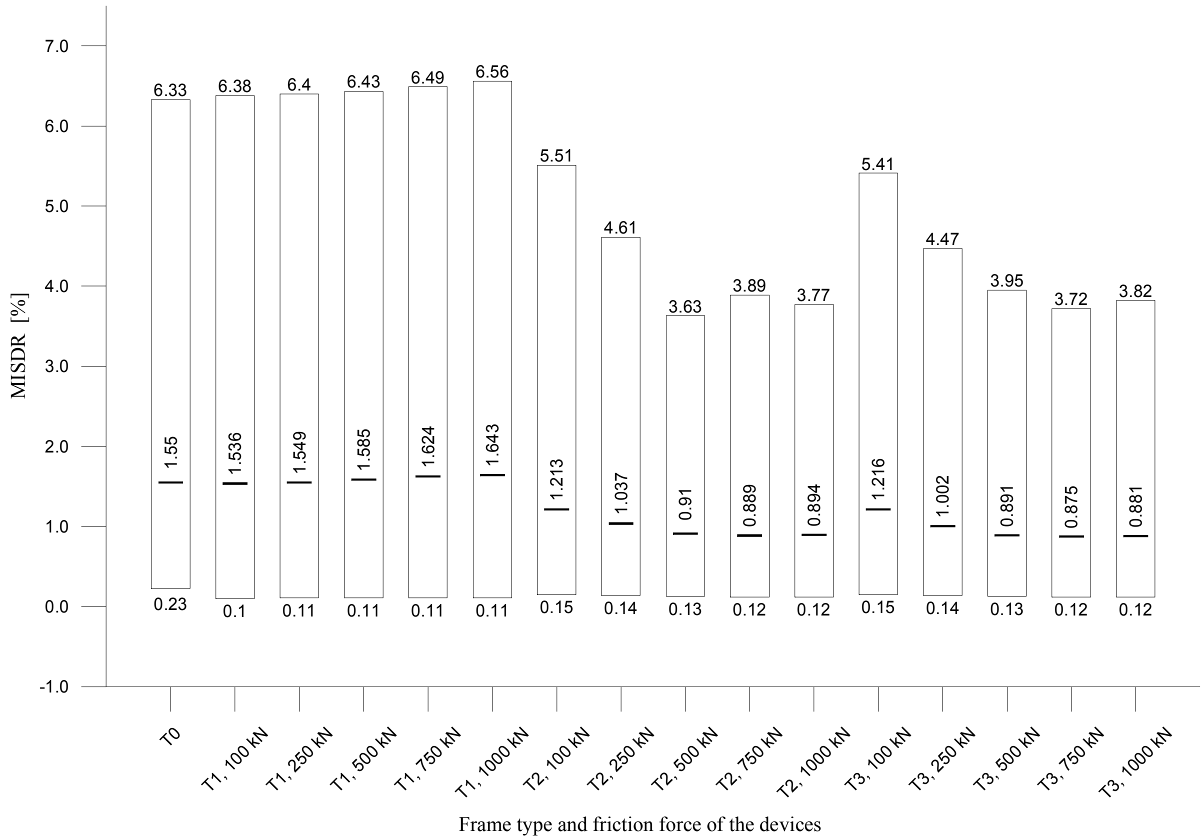

Figure 4. MISDR in relation with the frame type and the friction force of the devices

Table 2. Tabular overview of the MISDR results

Frame type and friction forces	**MISDR [%]**			**MISDR value difference (as % of frame type 0)**			**MISDR final value (as % of frame type 0)**		
	Maximum	**Minimum**	**Mean**	**Maximum**	**Minimum**	**Mean**	**Maximum**	**Minimum**	**Mean**
T0	6.330	0.230	1.550	0.000	0.000	0.000	100.00	100.00	100.00
T1, 100 kN	6.380	0.100	1.536	-0.790	56.522	0.903	100.790	43.478	99.097
T1, 250 kN	6.400	0.110	1.549	-1.106	52.174	0.065	101.106	47.826	99.935
T1, 500 kN	6.430	0.110	1.585	-1.580	52.174	-2.258	101.580	47.826	102.258
T1, 750 kN	6.490	0.110	1.624	-2.528	52.174	-4.774	102.528	47.826	104.774
T1, 1000 kN	6.560	0.110	1.643	-3.633	52.174	-6.000	103.633	47.826	106.000
T2, 100 kN	5.510	0.150	1.213	12.954	34.783	21.742	87.046	65.217	78.258
T2, 250 kN	4.610	0.140	1.037	27.172	39.130	33.097	72.828	60.870	66.903
T2, 500 kN	3.630	0.130	0.910	42.654	43.478	41.290	57.346	56.522	58.710
T2, 750 kN	3.890	0.120	0.889	38.547	47.826	42.645	61.453	52.174	57.355
T2, 1000 kN	3.770	0.120	0.894	40.442	47.826	42.323	59.558	52.174	57.677
T3, 100 kN	5.410	0.150	1.216	14.534	34.783	21.548	85.466	65.217	78.452
T3, 250 kN	4.470	0.140	1.002	29.384	39.130	35.355	70.616	60.870	64.645
T3, 500 kN	3.950	0.130	0.891	37.599	43.478	42.516	62.401	56.522	57.484
T3, 750 kN	3.720	0.120	0.875	41.232	47.826	43.548	58.768	52.174	56.452
T3, 1000 kN	3.820	0.120	0.881	39.652	47.826	43.161	60.348	52.174	56.839

Table 2 shows explicitly the maximum, the minimum and the mean values of MISDR, for all the examined frame types and all the friction forces. In addition, Table 2 shows their percentile difference from the respective values of frame type 0. Their final values as percentage of the respective values of frame type 0 are also exposed. Frame type 0 represents the case without friction dampers. From this Table is obvious that the maximum, the minimum and mean values reduce up to 42.654% (T2, 500kN), 47.826% (T2, T3, 750 kN, 1000 kN) and 43.548% (T3, 750 kN). The respective final MISDR values are equal to 57.346%, 52.174% and 56.452% of the initial one (without friction damper), respectively.

7. CONCLUSIONS

This paper investigated the seismic behavior of a ten-story steel frame with friction devices. Different absorber topologies and different friction forces were considered. The maximum inter-story drift ratio was utilized for the description of the postseismic damage status of the structure. This global damage indicator was computed by means of nonlinear dynamic analyses for a set of 66 recorded accelerograms. The results show the damage-reducing effect of the friction absorbers. The best response was provided by the frame type 2 (friction absorbers in all stories) and the frame type 3 (friction devices in all stories except the ground floor) with friction forces in the absorbers of 750 kN. In this case the mean value of the used damage indicator decreased up to 43.548%. In addition, the extreme values of the MISDR decreased up to 47.826%.

REFERENCES

Butterworth, J.W. (1999). Seismic Response of Steel Frames Containing Hierarchical Friction-Dissipating Joints, *Mechanics of Structures and Materials*, Bradford, Bridge & Foster (eds), Balkema, Rotterdam, 551-556.

Constantinou, M.C., Soong, T.T. and Dargush, G.F. (1998). Passive Energy Dissipation Systems for Structural Design and Retrofit, *MCEER Monograph Series No 1*, State University of New York, Buffalo.

Elenas, A. and Meskouris, K. (2001). Correlation study between seismic acceleration parameters and damage indices of structures, *Engineering Structures* **23:6**, 698-704.

Fitzgerald, T. F., Anagnos, T., Goodson, M. and Zsutty T. (1989). Slotted Bolted Connections in Aseismic Design for Concentrically Braced Connections, *Earthquake Spectra* **5:2**, 383-391.

Hanson, R.D. and Soong, T.T. (2001). Seismic Design with Supplemental Energy Dissipation Devices, *Monograph Series* **8**, EERI, Oakland, California.

Li, C. and Reinhorn, A.M. (1995). Experimental and Analytical Investigation of seismic Retrofit of Structures with Supplemental Damping: Part II - Friction Devices, *Report NCEER-95-0009*, State University of New York, Buffalo.

Meskouris, K. (2000). Structural Dynamics, Ernst & Sohn, Berlin.

Valles, R., Reinhorn, A.M., Kunnath, S.K., Li, C. and Madan, A. (1996). IDARC 2D Version 4.0: A program for the Inelastic Damage Analysis of Buildings, *Technical Report NCEER-96-0010*, State University of New York, Buffalo.